Organization of Acetylcholine Receptor Clusters in Cultured Rat Myotubes Is Calcium Dependent

SHERRY BURSZTAJN, JAMES L. McMANAMAN, and STANLEY H. APPEL
Department of Neurology, Neuroscience Program, Jerry Lewis Neuromuscular Disease Research Center, Baylor College of Medicine, Houston, Texas 77030

ABSTRACT The effect of extracellular Ca^{2+} concentration and myasthenic globulin on the distribution and appearance of acetylcholine receptor (AChR) clusters on rat myotubes was studied with tetramethyl-rhodamine-labeled αBTX. Low Ca^{2+} medium (2.5×10^{-5} M) caused a time-dependent loss of AChR clusters, and a concomitant increase in small punctate areas of fluorescence. High Ca^{2+} concentrations (1.5×10^{-2} M) increased the size of AChR clusters without altering AChR synthesis. These changes were not observed with other divalent ions. In the presence of myasthenic globulin, the rate of AChR turnover increases, and AChR clusters are rapidly dispersed. High Ca^{2+} concentration partially protects the AChR clusters from dispersal and decreases the rate of receptor turnover.

In cultured myotubes, acetylcholine receptors (AChR)[1] appear over the entire muscle surface. Both clustered and diffuse AChR are found on noninnervated myotubes derived from neonatal rat or embryonic chick muscle (3, 4, 5, 7, 22, 39). The diffuse receptors are laterally mobile. The diffusion constant for these receptors (5×10^{-11} cm^2/s), measured by the photobleaching recovery technique (4), is consistent with a freely diffusible macromolecule. In contrast, clustered receptors are essentially immobile and tightly packed with densities of $\sim 5 \times 10^3/\mu$m (4). It is not known whether the clustered AChR are formed from diffuse receptors, or whether the clustered receptors constitute an independent population of AChR that are inserted into specialized domains on the surface of myotubes. The diffuse AChR can contribute toward cluster formation (2); however, in some cases direct insertion of newly synthesized AChR into the plasma membrane has also been implicated (38).

Some of the factors that influence cluster stability are beginning to be identified; metabolic inhibitors and low concentration of extracellular calcium lead to the loss of AChR clusters (7, 9). This loss of receptor clusters was thought to be due to the dispersion of clusters, since the appearance of the clusters changes gradually from large areas of intense fluorescence to loosely organized patches of fluorescence, and finally to the complete loss of all fluorescent patches. However, metabolic inhibitors and low concentrations of calcium also decrease the rate of AChR synthesis (6, 28, 37). Thus, the changes in AChR clusters could be secondary to an effect on AChR metabolism.

We have recently shown that the addition of myasthenic globulin (MG) to cultured rat myotubes leads to a rapid loss of AChR clusters with a corresponding increase in the number of small (2–6 μm in diameter) fluorescent patches (microaggregates) (13). The loss of clusters produced by MG occurs at a rate greater than the overall rate of turnover of AChR, indicating that MG interacts directly with AChR leading to cluster dispersal.

The influence of agents that affect AChR clusters is complicated by their effects on AChR metabolism. Therefore, it is important to investigate the regulation of clusters under conditions in which there is little influence on AChR metabolism. We studied the role of high Ca^{2+} concentration on the number and size of AChR clusters. High concentrations of Ca^{2+}, contrary to the report in other species (6), do not have a significant effect on AChR metabolism but do influence cluster size. We have also investigated the influence of high concentrations of Ca^{2+} on the loss of receptors produced by MG.

MATERIALS AND METHODS

Culture Condition and Medium Preparation: Primary cultures were prepared from hind limbs of neonate Sprague-Dawley rats, as described by Yaffe (40). Dissociated muscle tissue was plated in Dulbecco-Vogt modified Eagle's medium (DME) containing 10% (vol/vol) horse serum (Grand Island Biological Co., Grand Island, NY), and 0.5% chick embryo extract (vol/vol),

[1] *Abbreviations used in this paper:* AChR, acetylcholine receptors; αBTX, α-bungarotoxin; DME, Dulbecco-Vogt modified Eagle's medium; MG, myasthenic globulin; TMR, tetramethyl rhodamine.

THE JOURNAL OF CELL BIOLOGY · VOLUME 98 FEBRUARY 1984 507-517
 · 0021-9525/84/02/0507/11 $1.00

200 mM glutamine, and 40 mg/ml, garamycin. Cells at a density of 5×10^5 per ml were plated into Falcon 35-mm petri dishes (Falcon Labware, Oxnard, CA) containing collagen-coated glass cover slips (Gold seal #1 thickness). Cultures were maintained at 37°C in an atmosphere of 95% air, 5% CO_2. Within 24–48 h after plating, cells attach to substratum, divide, and fuse with one another, forming long multinucleated myotubes. The culture medium was changed every 2 d. All experiments were performed on day 6 or 7 after plating.

Low Ca^{2+} medium was prepared from Ca^{2+}-free DME supplemented with horse serum dialyzed against Ca^{2+}-free phosphate buffered saline. High Ca^{2+} medium was prepared similarly, except that a known concentration of calcium was added. The final concentration of Ca^{2+} in the medium was determined by atomic absorption spectroscopy. Medium containing 1.8×10^{-3} M Ca^{2+} and supplemented with 1.5×10^{-2} M of $MgCl_2$ or $SrCl_2$ was used to determine whether the effects observed at various Ca^{2+} concentrations can be mimicked by other divalent ions.

Localization of AChR Clusters: α-Bungarotoxin (αBTX) was conjugated to monotetramethylrhodamine (TMR) as described by Ravdin and Axelrod (33). Labeled αBTX was separated from free TMR by chromatography on Sephadex G-25 in 0.10 mM sodium phosphate, pH 7.0. The excluded fluorescent peak was placed on a carboxymethyl CM-Sephadex C-50 cation-exchange column and eluted with sodium chloride in sodium phosphate buffer. Optical densities and absorbance spectra were determined on a spectrophotometer. The specificity of the αBTX-TMR (5×10^{-8} M) was determined by

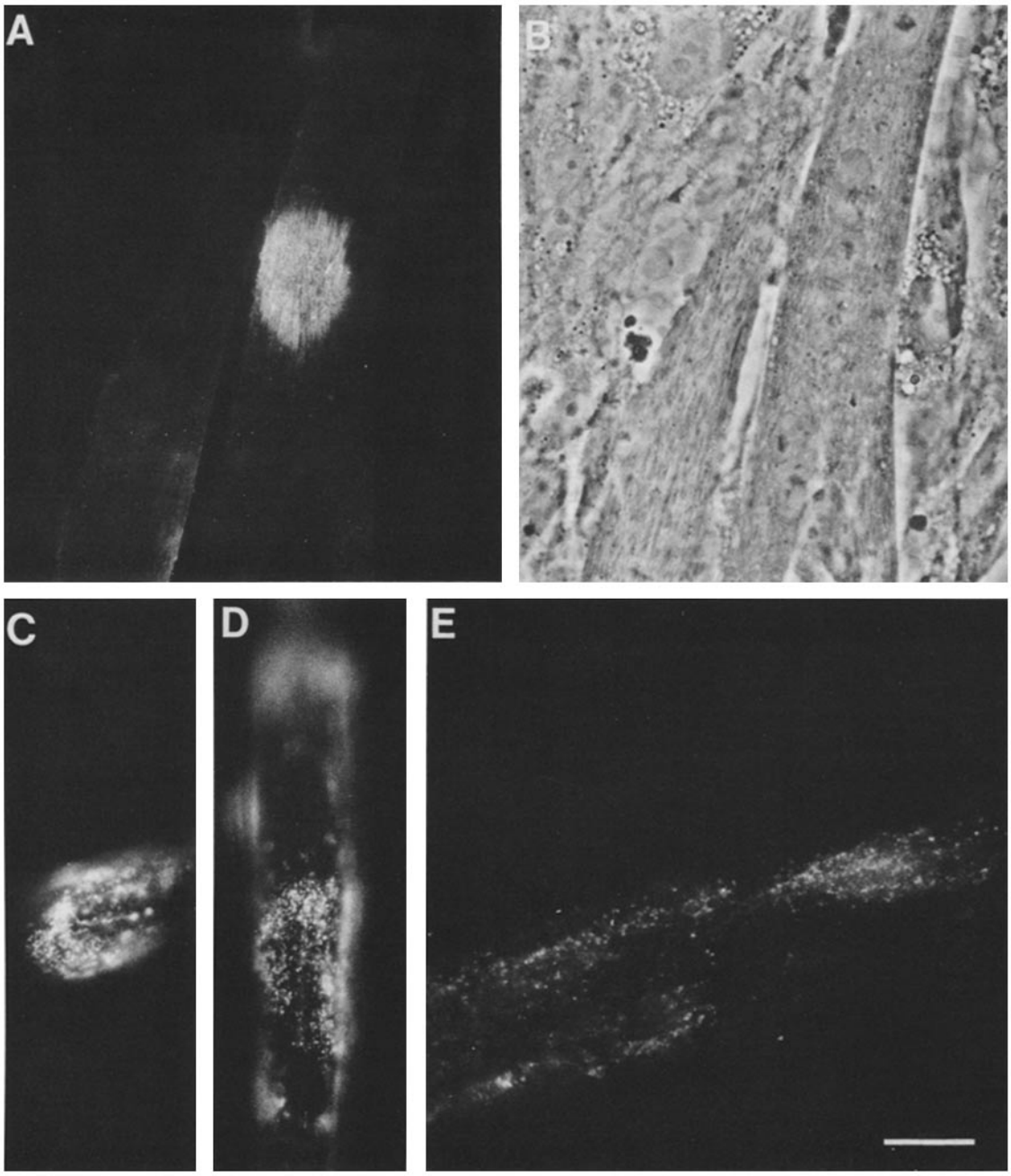

FIGURE 1 Control and low Ca^{2+} (2.5×10^{-5} M) incubated myotubes after staining with fluorescent αBTX. Rat myotubes were grown on collagen-coated coverslips, washed, and incubated with culture medium containing low Ca^{2+} for 3–24 h. Cells were washed with HBSS, stained with αBTX-TMR as described in Materials and Methods, and fixed in 1% phosphate-buffered formaldehyde. (*A*) Control myotubes showing an intensely fluorescent AChR cluster. Strands of fluorescence radiate through the cluster. (*B*) Phase-contrast image of the same myotube as in *A* showing that the AChR cluster is located over nuclei. (*C*) Myotube incubated at low Ca^{2+} concentration for 6 h. (*D*) 12-h incubation in low Ca^{2+}. (*E*) 24-h incubation in low Ca^{2+}. A progressive breakdown of AChR clusters as seen by the appearance of speckles (*C–E*). All photographs were exposed and printed identically. Bar, 25 μm. × 480.

incubating myotubes with unlabeled αBTX (5×10^{-8} M for 1 h) followed by incubation in αBTX-TMR (1 h at 37°C in DME). <10% of surface AChR are internalized in 1 h (12). No fluorescent label was seen in toxin-blocked cultures. Cultures incubated in αBTX-TMR showed intensely fluorescent clusters. Cells grown on glass coverslips were fixed in 2% formaldehyde in 0.1 M sodium phosphate buffer (15). A drop of glycerin sodium phosphate solution diluted 9:1 was placed beneath the glass coverslip. Cells were observed with a Zeiss fluorescence microscope equipped with epiillumination. Photographs were taken at ASA 800 with Tri-X film at total magnification of × 400, unless otherwise stated.

Quantitation of Fluorescence AChR Distribution and Dimensions of Clusters: Cultures were examined in order to determine the percentage of intact AChR clusters, diffuse AChR, and microaggregates.

TABLE I

AChR Cluster Distribution in Low Ca^{2+} Medium

Incubation time in low Ca^{2+} medium	Intact AChR clusters	AChR cluster dimension
h	%	*μm*
0	90.5 ± 5.2	38.2 ± 5.0 (62)
3	80.7 ± 7.6	32.9 ± 6.2 (60)
6	43.3 ± 9.0	31.3 ± 6.4 (62)
12	44.6 ± 6.6	30.5 ± 6.9 (57)
24	34.7 ± 7.0	31.6 ± 5.1 (50)

Loss of AChR clusters and decrease in cluster size after incubation in low Ca^{2+} medium (2.5×10^{-5} M). 20 fields containing 50–60 myotube segments in each culture were viewed, and the numbers of intact and dispersed AChR clusters (as stated in Materials and Methods) were counted. The number of intact AChR remaining is expressed as a percentage of total AChR cluster ± SD in each of three cultures. The number in parentheses represents the number of myotube segments scored.

TABLE II

Reappearance of AChR Clusters on Myotubes after Transfer to Ca^{2+}-Containing Medium

Incubation time in Ca^{2+}-containing (1.8 mM) medium	Intact AChR clusters	AChR cluster dimensions
h	%	*μm*
0	34.7 ± 7.0	31.6 ± 5.1 (50)
3	50.0 ± 7.7	33.1 ± 8.7 (55)
6	55.1 ± 7.1	36.7 ± 9.2 (55)
12	70.3 ± 7.5	36.3 ± 6.4 (45)
24	78.8 ± 7.1	42.3 ± 8.9 (49)

Cultures were incubated in low Ca^{2+} medium for 24 h after which they were switched to control Ca^{2+}-containing medium (1.8×10^{-3} M) for the time-periods indicated above. Control cultures incubated in the continuous presence of 1.8×10^{-3} M Ca^{2+} contain 90.6% ± 5.2 of intact AChR clusters. The number of intact AChR clusters remaining is expressed as a percentage of total clusters ± SD. The mean AChR cluster size ± SD is stated. The parentheses show the number of myotube segments scored in each of three cultures.

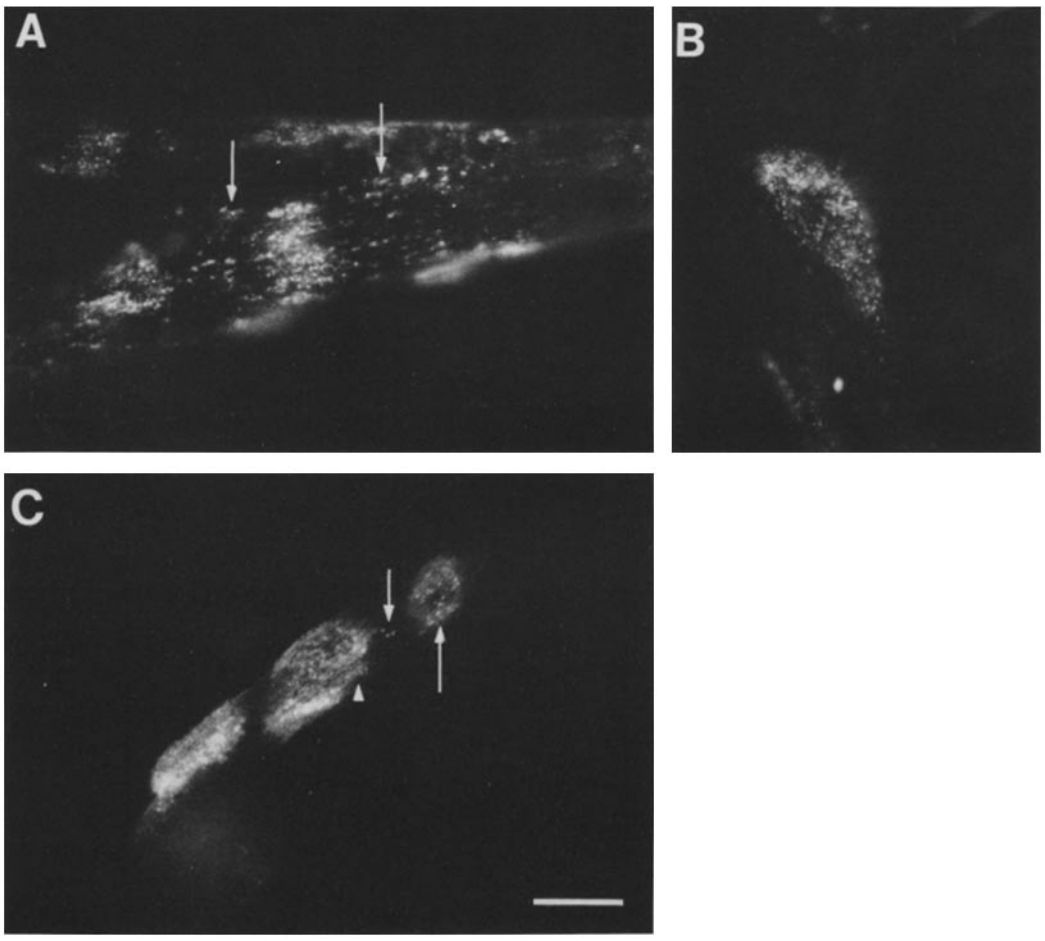

FIGURE 2 Reappearance of AChR clusters following incubation in low Ca^{2+} medium (2.5×10^{-5} M) for 24 h and transfer to control Ca^{2+} medium for time-periods indicated. Cells were stained with αBTX-TMR as described in Fig. 1. (*A*) Fluorescent image on myotubes 3 h after removal from low Ca^{2+} medium and incubation in control Ca^{2+} medium. Fluorescent speckles (arrows) are seen scattered on the myotube. (*B*) Myotube 6 h after incubation in low Ca^{2+} medium and transfer to control Ca^{2+} medium. An AChR cluster with fluorescent speckles is present. (*C*) 12 h after transfer from low Ca^{2+} medium to control Ca^{2+} medium, AChR cluster topography begins to resemble that of controls. Speckles (arrows) and strands (arrowheads) are present. All photographs were exposed and printed identically. Bar, 25 μm. × 480.

Only AChR clusters that had discrete patches of fluorescence not present on overlapping cells and confined only to an intact myotube (not a damaged cell or membrane fragments) were scored as intact clusters (e.g., Fig. 1*A*). Under normal culture conditions, myotubes have large AChR clusters with an average length of 38 μm and small clusters of receptors with lengths of 2–6 μm, called microaggregates. These microaggregates appear under the fluorescence microscope as small "speckles" (Fig. 1*E*) and are easily distinguished from the larger AChR clusters (13). A dispersed cluster was defined as a fluorescent patch, no longer intact, containing microaggregates (e.g., Fig. 1, *C* and *D*). Cluster dimensions were expressed in micrometers of cluster length as previously reported (3, 41). Random microscopic fields were examined, and the number of myotubes containing intact AChR clusters and the number of myotubes containing microaggregates were counted. Myotubes that appeared branched were scored as one myotube. At least 40 myotubes per culture were examined, and the data were expressed as a percentage of total myotube segments that had intact AChR clusters as previously described (13). The number of AChR clusters per myotube was determined and expressed as a ratio of AChR clusters/myotube. All experiments were carried out in duplicates and repeated at least three times.

TABLE III

AChR Cluster Distribution in High Calcium Medium

Incubation time	Intact AChR clusters	AChR cluster dimensions
h	%	*μm*
0	91.0 ± 4.0	34.2 ± 4.5 (85)
3	91.6 ± 3.6	33.4 ± 3.6 (87)
6	92.5 ± 3.6	35.5 ± 8.7 (81)
12	94.1 ± 3.3	45.0 ± 13.3 (82)
24	95.5 ± 2.4	56.0 ± 13.4 (81)

AChR cluster distribution and their dimensions following incubation in high calcium medium (1.5×10^{-2} M) at the stated time intervals. The number of intact AChR clusters is expressed as a percentage of total AChR clusters counted ± SD. The AChR cluster dimensions are expressed as a mean ± SD of 20 microscopic fields. The parentheses represent the number of myotube segments containing AChR clusters scored in each of three cultures.

TABLE IV

Effect of Ca^{2+} on the Synthesis and on the Number of Surface AChR

Time	1.8×10^{-3} M Ca^{2+}	1.5×10^{-2} M Ca^{2+}
h		
9	5,416 ± 199	6,322 ± 384
24	11,154 ± 480 (15,824 ± 842)	11,419 ± 374 (17,253 ± 1,188)

The number of new AChR and the number of total surface AChR (numbers in parentheses) are not significantly different from those of control cultures following incubation for 24 h in high Ca^{2+} medium. Myotubes were incubated with unlabeled αBTX (1×10^{-8} M) for 1 h, washed three times with Hank's basic salt solution, and incubated with ^{125}IαBTX at 0 h, 9 h, and 24 h after washing and incubation in culture medium. The 0-h values were subtracted from the values presented. The values represent the mean ± SD of duplicate cultures in each of three experiments.

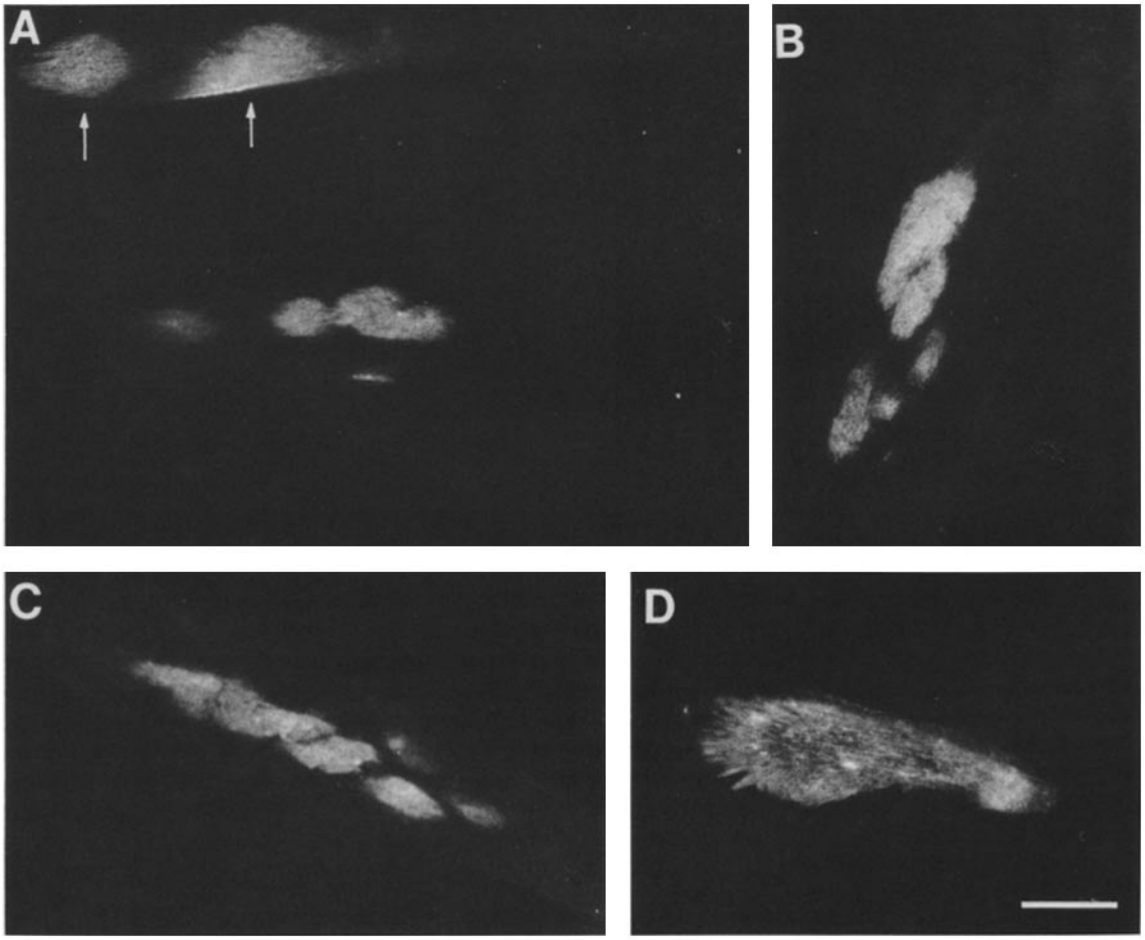

FIGURE 3 The distribution of AChR clusters after incubation of rat myotubes in culture medium containing high Ca^{2+} (1.5×10^{-2} M). Cells were stained with αBTX-TMR as described in Fig. 1. (*A*) Fluorescent images of AChR clusters on myotubes 6 h after incubation in high Ca^{2+} medium. Multiple clusters on myotubes close to one another are present (arrows). (*B*) 12 h after incubation with high Ca^{2+} medium, a further increase in the number of AChR clusters close to one another is seen. (*C–D*) 24 h after incubation with high Ca^{2+} medium. Large AChR clusters close to each other and (*D*) clusters with no discontinuity within the cluster are also present. All photographs were developed and printed identically. Bar, 25 μm. × 480.

Quantitation of AChR Using [^{125}I]αBTX: AChR surface levels and the rates of synthesis and degradation were determined using [^{125}I]αBTX as described by Devreotes and Fambrough (17). Surface AChR were measured by incubating cells with 2×10^{-8} M [^{125}I]αBTX (50–150 Ci·mmol^{-1}) for 1 h after exposure to 1.8–15 mM Ca^{2+} DME. Cultures were washed four times with Hanks' balanced salt solution containing 0.1% bovine serum albumin to remove the unbound toxin and extracted with 50 mM Tris, pH 7.4, 50 μM NaCl, and 1% Triton X-100. Cells were removed from the dishes with a rubber policeman, and samples were centrifuged at 15,000 *g* for 15 min to remove debris, and counted in a gamma counter. Background counts were determined by pretreatment of cells with unlabeled αBTX (5×10^{-7} M) followed by incubation with [^{125}I]αBTX. The background counts were found to be 10–15% of total bound counts. The rate of appearance of new AChR in the plasma membrane was determined by incubating cells with unlabeled αBTX (5×10^{-7} M) for 1 h to block the existing surface AChR. Cells were washed with DME to remove the unbound unlabeled αBTX and incubated with DME containing the specified concentration of Ca^{2+} for 3–24 h, following which the cells were exposed to [^{125}I]αBTX and quantitated as described above. This procedure allows for only the newly synthesized AChR to be counted (17).

The AChR rate of degradation was determined by prelabeling the cells with [^{125}I]αBTX. Cells were washed to remove unbound [^{125}I]αBTX, fresh medium containing 1.8–15 mM Ca was added, and the amount of [^{125}I]αBTX remaining was determined at selected time points over a 24-h period. αBTX binds to the AChR essentially irreversibly with a one-half time-period for dissociation of ~1 wk. The AChR turnover rate was also determined in the presence of MG (5 mg/ml) and normal globulin after incubation with 1.8–15 mM Ca^{2+}-containing DME.

Purification of Globulin: The globulin fraction from normal and myasthenic serum was purified by three cycles of ammonium sulfate precipitation according to the procedure of Deutsch (16). The redissolved globulin was dialyzed against 10 mM phosphate buffer, pH 7.0, lyophilized, and stored at −70°C.

RESULTS

Loss of AChR Clusters Following Incubation in Low Ca^{2+} Medium

Cultured rat myotubes contain clusters of AChR (3, 7) that can be stained using αBTX conjugated to the fluorescent dye TMR. Rat myotubes incubated in medium containing 1.8 mM Ca^{2+} and stained with αBTX-TMR display brightly fluorescent AChR clusters (Fig. 1*A*). These clusters have a length of 36.3 ± 8 μm (mean ± SD) and exhibit strands that run through the clusters (Fig. 1*A*). As previously reported for chick myotubes, the rat AChR clusters are also frequently found over the nuclear region of the myotube (23).

The number of AChR clusters per culture increases with time, usually reaching a plateau 7–8 d after plating. Under normal culture conditions the clusters are stable; however, when the Ca^{2+} concentration of the medium was reduced to 2.5×10^{-5} M, a condition that has previously been shown to disrupt AChR clusters (7), a loss of AChR clusters was observed. The loss of clusters was quantitated by determining

TABLE V

Effect of Divalent Ions on AChR Cluster Distribution

Addition of divalent ions	Incubation time	Intact AChR clusters	AChR cluster dimensions
	h	%	*μm*
High $CaCl_2$	24	94.1 ± 4.2	52.3 ± 14.5 (67)
High $CaCl_2$	48	93.4 ± 5.3	53.8 ± 13.2 (64)
Control $CaCl_2$	24	92.0 ± 4.4	37.7 ± 6.7 (65)
Control $CaCl_2$	48	89.4 ± 5.4	37.6 ± 5.0 (68)
$MgCl_2$	24	93.0 ± 3.9	35.3 ± 4.3 (67)
$MgCl_2$	48	92.3 ± 4.3	36.5 ± 5.8 (69)
$SrCl_2$	24	89.7 ± 4.9	32.9 ± 3.4 (65)
$SrCl_2$	48	89.5 ± 5.0	33.6 ± 6.9 (64)

Distribution of AChR clusters and their dimensions after exposure of cultured myotubes to a medium to which divalent ions (1.5×10^{-2} M) were added. The number of intact AChR clusters remaining is expressed as a percentage of total AChR clusters ± SD. The AChR cluster dimensions are expressed as a mean ± SD. High $CaCl_2$ indicates culture medium containing 1.5×10^{-2} M $CaCl_2$. Control $CaCl_2$ indicates culture medium containing 1.8×10^{-3} M $CaCl_2$. The parentheses show the number of myotube segments scored.

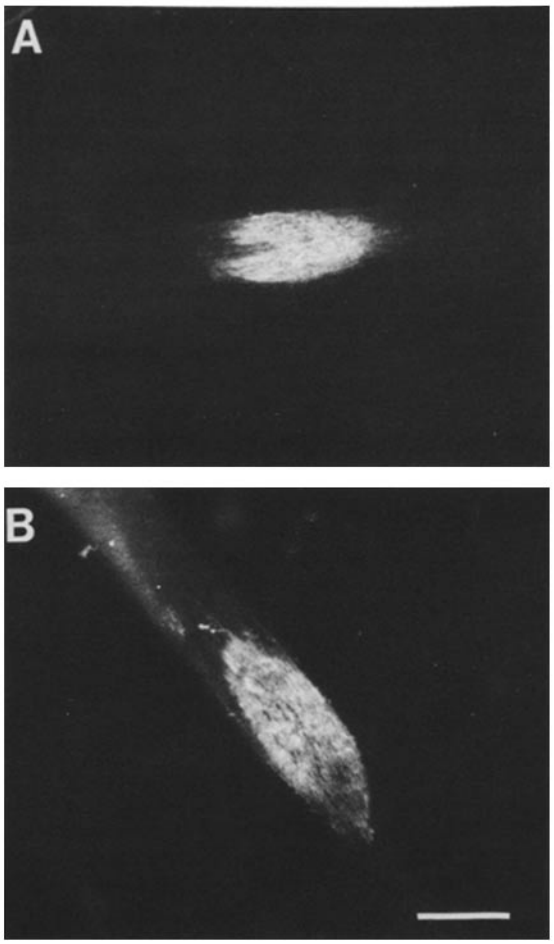

FIGURE 4 Incubation of cultures with other divalent ions 1.5×10^{-2} M (*A*) $MgCl_2$ or (*B*) $SrCl_2$ in the presence of 1.8×10^{-3} M Ca^{2+} has no effect on the morphological distribution of AChR clusters. All photographs were developed and printed identically. Bar, 25 μm. × 480.

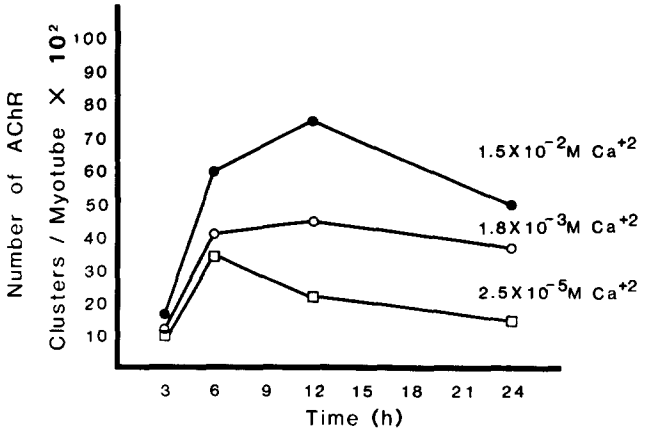

FIGURE 5 The distribution ratio of newly formed AChR clusters: the number of intact clusters per myotube. 50 myotubes in duplicate cultures containing AChR clusters were counted for each time-point. The highest ratio of clusters per myotube is present after incubation in 1.5×10^{-2} M Ca^{2+}-containing medium for 12 h.

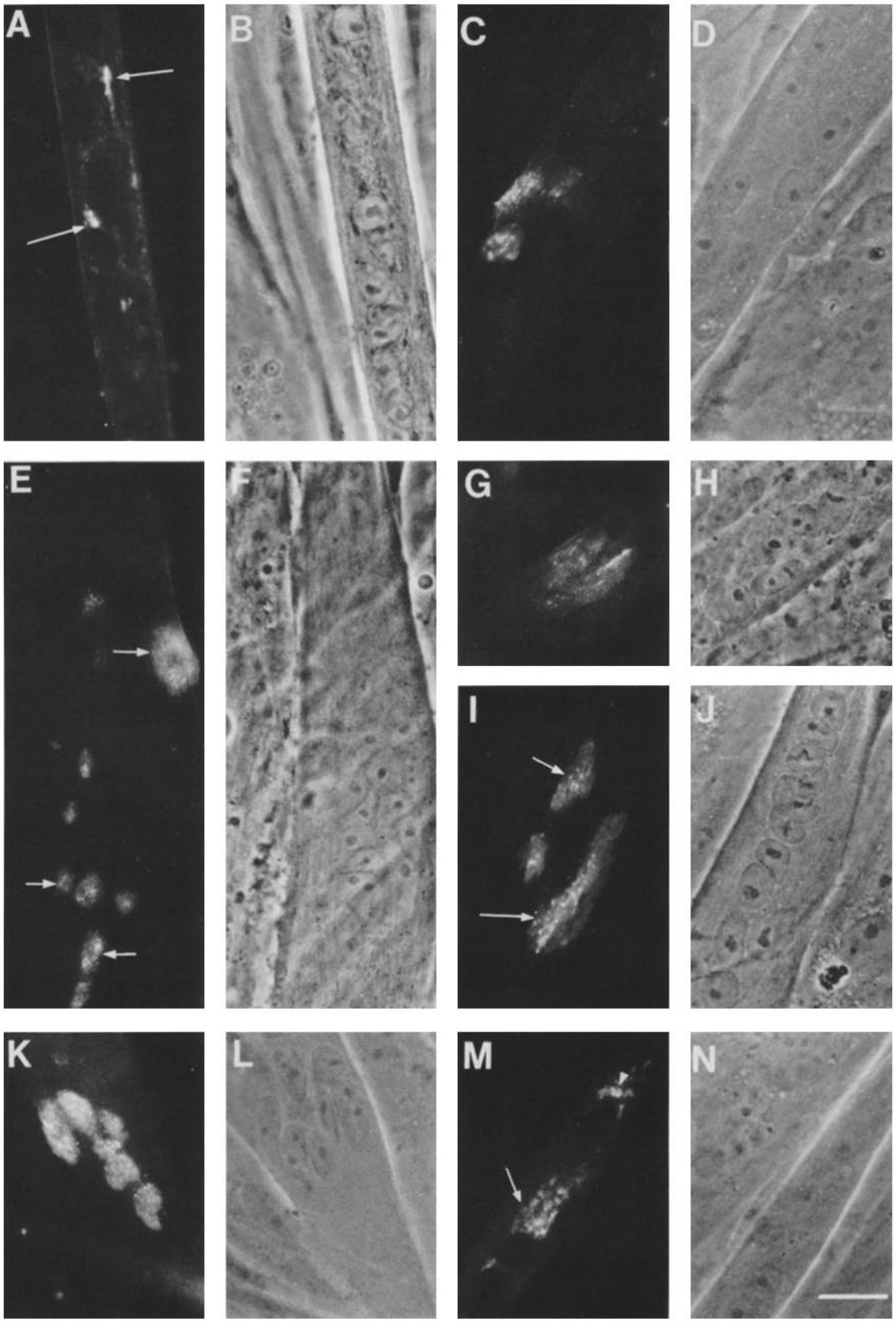

FIGURE 6 *De novo* formation of AChR incubated in culture medium containing control (1.8×10^{-3} M), high (1.5×10^{-2} M), and low (2.5×10^{-5} M) levels of Ca^{2+}. Cells were incubated with unlabeled αBTX for 1 h, washed, and stained with αBTX-TMR as described in the experimental section. (*A*) 3 h after removal of unlabeled αBTX, small fluorescent aggregates (arrows) begin to appear at all three Ca^{2+} concentrations tested. (*B*) Phase-contrast image of (*A*). (*C* and *D*) Myotubes incubated in control Ca^{2+} medium for 6 h. (*C*) Fluorescent aggregates containing small, intensely fluorescent speckles. (*D*) Phase-contrast image of the same myotube as in *C*. (*E* and *F*) Myotubes incubated in high Ca^{2+} medium for 6 h. (*E*) Multiple fluorescent clusters on the same myotube (arrows) close to one another are present. (*F*) The morphology of myotubes as seen with the phase-contrast microscopy remains unchanged. (*G* and *H*) Myotubes incubated in low Ca^{2+} medium for 6 h. (*G*) Fluorescent image of an AChR cluster showing a mottled appearance. (*H*) Phase-contrast image of *G*. (*I* and *J*) Myotubes incubated in control Ca^{2+} medium for 12 h.

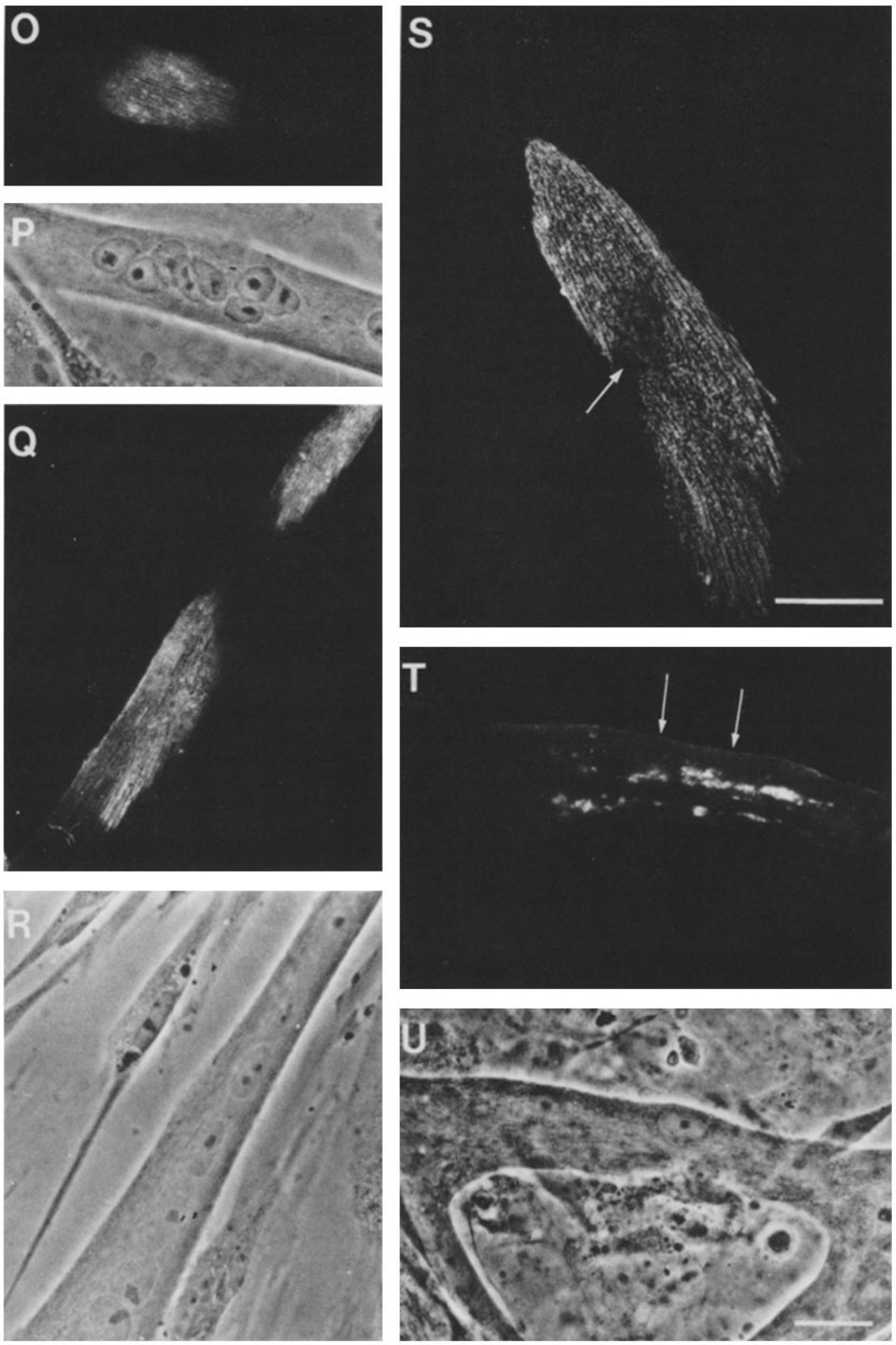

(*I*) Multiple AChR clusters close to one another with intensely fluorescent speckles (arrows) are present. (*J*) Phase-contrast image of the same myotube as in (*I*). (*K* and *L*) Myotubes incubated in high Ca^{2+} medium for 12 h. (*K*) Fluorescent aggregates, some of which give the appearance of continuity with one another, are present. (*L*) Phase-contrast image of *K*. (*M* and *N*) Myotubes incubated in low Ca^{2+} medium for 12 h. (*M*) AChR cluster showing nonuniform fluorescence within the cluster (arrow). Small aggregates with intensely fluorescent speckles are also present (arrowhead). (*N*) Phase-contrast image remains unchanged. (*O* and *P*) Myotubes incubated in control Ca^{2+} medium for 24 h. (*O*) A fluorescent AChR cluster contains strands and speckles. (*P*) Phase-contrast image of *O* shows that the AChR cluster is localized over nuclei. (*Q–S*) Myotubes incubated in high Ca^{2+} medium for 24 h. (*Q*) Fluorescent images of large AChR clusters close to one another are present. (*R*) Phase-contrast image of the myotube in *Q* remains unchanged. (*S*) Higher magnification of a fluorescent AChR cluster showing a less intensely fluorescent area in the center of the cluster (arrow). (*T* and *U*) Myotubes incubated in low Ca^{2+} medium for 24 h. (*T*) Intensely fluorescent microaggregates aligned with the long axis of the myotube (arrows). (*U*) Phase-contrast image of the myotube in *T* remains unchanged. All photographs were developed and printed identically. *A–R* and *T–U*, × 480; *S*, × 705. Bar, 25 μm.

the percentage of intact clusters remaining after incubation in normal or low Ca^{2+} medium (see Materials and Methods). We found that, following incubation in low Ca^{2+} medium, there was a time-dependent decrease in the number of AChR clusters (Table I) as well as changes in the cluster appearance. Incubation in low Ca^{2+} medium for 6 h decreased the number of intact clusters to <50% of the starting value. The remaining clusters have lost the strands that were initially apparent and have a nonuniform appearance (Fig. 1 *C*). By 12 h the AChR clusters have become more diffuse, although small speckles remain (Fig. 1 *D*). After 24 h, most of the AChR clusters have been replaced by fluorescent speckles, which are distributed randomly throughout the surface of the myotubes (Fig. 1 *E*). It is difficult to objectively quantify the degree of cluster dispersal because of the variability between these categories, and thus these quantitations were not carried out.

The effect of low Ca^{2+} concentration was reversible. Myotubes incubated in low Ca^{2+} medium for 24 h and then switched to control medium containing 1.8×10^{-3} M Ca^{2+} showed a gradual reappearance of AChR clusters (Table II). 3 h after transfer to control medium, intensely fluorescent speckles close to one another are seen (Fig. 2 *A*). 6 h after transfer to control medium the AChR speckles are confined to the cluster (Fig. 2 *B*), and the random distribution of fluorescence is no longer seen. By 12 h, the AChR clusters are indistinguishable from those of control cells (Fig. 2 *C*). Thus, incubation in low Ca^{2+} medium does not irreversibly damage the myotubes, or impair the formation of clusters.

Distribution of AChR Clusters at High Ca^{2+} Concentrations

Since low Ca^{2+} concentration in the medium causes the loss of intact AChR clusters, we have examined the possibility that high Ca^{2+} medium (1.5×10^{-2} M) may promote AChR cluster formation. During the first 3 h of incubation in high Ca^{2+} medium, there was no change in cluster dimensions or in the percentage of intact clusters (Table III). Longer incubation periods resulted in a progressive increase in cluster dimensions (Table III); by 12 h, the myotubes have developed multiple clusters close to each other (Fig. 3, *A* and *B*). By 24 h, there is a 61% increase in the length of the average cluster (Table III), but the fluorescence of the cluster is still not uniform (Fig. 3 *C*). There are, however, a few large clusters that are uniformly stained (Fig. 3 *D*). The increase in cluster dimensions may be the result of an increase in AChR lateral diffusion, allowing diffuse AChR to fuse with existing AChR clusters, or to an increased rate of insertion of new AChR. Although the rate of AChR synthesis has been shown to be dependent on the concentration of extracellular Ca^{2+} for Ca^{2+} concentrations below 2×10^{-3} M (28), higher concentrations of extracellular Ca^{2+} did not affect the rate of AChR synthesis (Table IV).

There are a number of observations that suggest that the rate of lateral diffusion of AChR is increased: (*a*) At earlier stages of incubation with medium containing high Ca^{2+} concentration, multiple AChR clusters appear on the same muscle fiber but are farther from one another. (*b*) Large AChR clusters, some of which are 90 μm with a mean length of 56.0 $\pm$ 13.4 μm ($\pm$ SD) (Table III), are observed only after 24 h of incubation and not at earlier times. (*c*) The large clusters that are seen 24 h after high Ca^{2+} incubation show some discontinuity as evidenced by small nonfluorescent regions within a cluster (Fig. 3 *C*).

The effects of high concentrations of Ca^{2+} are specific. Elevated concentrations of other divalent ions such as $MgCl_2$ or $SrCl_2$ (1.5×10^{-2} M in the presence of 1.8×10^{-3} M Ca^{2+}) have no effect on the percentage of intact clusters, AChR cluster dimensions (Table V), or on AChR cluster morphology (Fig. 4, *A* and *B*).

Appearance of New AChR Clusters

To determine whether changes in Ca^{2+} concentration have an effect on the appearance of newly synthesized AChR, we incubated cultures with unlabeled αBTX (5×10^{-7} M) for 1 h in culture medium, washed, and incubated for 0 to 24 h in culture medium containing one of three concentrations of calcium: 2.5×10^{-5} M; 1.8×10^{-3} M; 1.5×10^{-2} M. The myotubes were then stained with αBTX-TMR to visualize receptor clusters. There was no difference in the percentage of intact AChR clusters on myotubes incubated with the various Ca^{2+} concentrations for up to 3 h. Thereafter, the number of clusters per myotube decreased for myotubes incubated in low Ca^{2+} medium, but continued to increase for myotubes incubated in normal and high Ca^{2+} medium (Fig. 5). 24 h after incubation in high Ca^{2+} medium, there is a decrease in AChR cluster number, which appears to coincide with the increase in cluster size (Table III). AChR clusters were not detected when cultures were stained with αBTX-TMR immediately after removal of unlabeled αBTX. These events are depicted in Fig. 6.

3 h after incubation at each of the three Ca^{2+} concentrations tested, small AChR clusters begin to appear which have similar dimensions and distribution on the myotube (Fig. 6 *A*). By 6 h, AChR clusters exhibit numerous speckles (Fig. 6, *C*, *E*, and *G*). Myotubes incubated in high Ca^{2+} have many more small clusters close to one another (Fig. 6 *E*) than myotubes incubated at the other concentrations. However, these myotubes do not yet contain the strands that are evident in untreated cultures (Fig. 1 *A*). Phase-contrast views of corresponding fluorescent images are seen in Fig. 6, *D*, *F*, and *H*.

The size of clusters on myotubes incubated in normal and high Ca^{2+} for 12 h continues to increase (Fig. 6, *I* and *K*), whereas clusters on myotubes incubated at low Ca^{2+} concentration decrease in size, with a marked disruption of clusters (Fig. 6 *M*). No obvious changes in the morphology of myotubes were seen at any of the calcium concentrations tested (Fig. 6, *J*, *L*, and *N*).

24 h after removal of unlabeled αBTX, cultures incubated in control medium have AChR clusters that are similar to those seen in untreated cultures. These AChR clusters contain strands (Fig. 6 *O*) that course through the cluster and have nuclei centered beneath them (Fig. 6 *P*). Myotubes incubated at high Ca^{2+} concentrations show AChR clusters that are larger than control (Fig. 6 *Q*). These clusters are also found over nuclei and, under higher magnification (Fig. 6 *S*), exhibit small weakly fluorescent areas that may represent fusion of clusters or clusters in the process of being filled in with diffuse AChR. Cultures incubated at low Ca^{2+} concentrations have few clusters (Fig. 5), and the majority of these are characterized by small fluorescent microaggregates (Fig. 6 *T*). The overall morphology of these myotubes remains identical to control (Fig. 6 *U*).

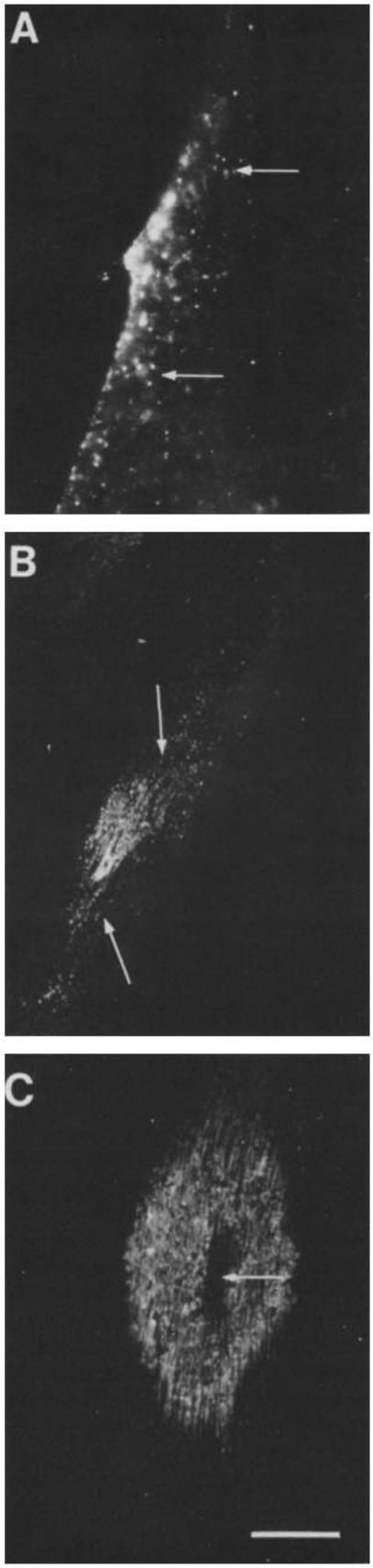

FIGURE 7 Distribution of AChR clusters on myotubes incubated with myasthenic globulin in control (1.8×10^{-3} M) or high Ca^{2+} (1.5×10^{-2} M) medium. Cultures were stained with αBTX-TMR as described in Fig. 1. (*A*) Myotubes incubated with MG for 6 h in control medium. Intensely fluorescent microaggregates (arrows) dispersed over the myotube are present. (*B* and *C*) Fluorescent images of myotubes that have been preincubated with high Ca^{2+} medium for 24 h and MG for 6 h. (*B*) Readily discernible AChR clusters surrounded by microaggregates (arrows) are present. (*C*) At times, AChR clusters devoid of fluorescence in the center of the cluster (arrow) are present. All photographs were exposed and printed identically. Bar, 25 μm. × 705.

TABLE VI

Distribution of AChR Clusters in the Presence of 15 mM Ca^{2+} and MG

Treatment	Intact AChR clusters	AChR cluster dimensions
	%	μm
None	90.6 ± 5.2	38.2 ± 7.4 (54)
MG globulin	18.1 ± 8.2	35.1 ± 5.2 (48)
15 mM Ca^{2+}	97.5 ± 2.4	53.1 ± 15.5 (47)
15 mM Ca^{2+} and MG	68.6 ± 7.8	45.1 ± 9.7 (47)

The distribution and size of AChR clusters on myotubes treated with myasthenic globulin in the presence of high Ca^{2+} concentration. Cultures were incubated with MG globulin for 6 h or preincubated for 24 h with medium containing high Ca^{2+} concentration (1.5×10^{-2} M) following which the cells were exposed to MG globulin for 6 h. The number of intact AChR clusters remaining is expressed as a percentage of total clusters ± SD. The numbers in parentheses show the number of cells scored in each of three cultures. The AChR cluster size is expressed as mean ± SD.

AChR Degradation Rate and AChR Cluster Stability after Exposure to MG

In normal Ca^{2+} medium the addition of MG produces a rapid decrease in the number of intact AChR clusters and increases the rate of AChR degradation leading to a decrease in total surface AChR (Fig. 7*A* and Table VI). However, when the Ca^{2+} concentration is increased to 1.5×10^{-2} M, the loss of intact AChR clusters (Table VI and Fig. 7, *B* and *C*) and the rate of AChR degradation are decreased (Fig. 8). The rate of AChR degradation in cultures treated with normal globulin was not affected by the concentration of Ca^{2+} in the medium (Fig. 8). These results suggest that dispersal of AChR clusters and degradation are linked to one another.

DISCUSSION

In muscle cells, the concentration of Ca^{2+}, in addition to its well known role in the regulation of muscle metabolism, may also regulate synthesis and degradation of AChR. The concentration of extracellular Ca^{2+} and pharmacological agents that alter intracellular Ca^{2+} levels have been shown to affect the rate of AChR synthesis but not degradation in cultured rat skeletal muscle (28, 37).

The concentration of extracellular Ca^{2+} also affects the number and morphology of AChR clusters. Calcium concentrations below 2×10^{-3} M lead to a loss of AChR clusters (9). This loss of clusters is partially explained by the decreased synthesis of AChR (28). However, the rapid decrease in the number of intact receptor clusters cannot be totally accounted for by a decreased rate of receptor synthesis, since the number of intact receptor clusters is reduced 50% after incubation of the myotube in low Ca^{2+} medium for 6 h, while the rate of appearance of new AChR (28) and the formation of new receptor clusters (Fig. 5) are not affected. These observations suggest that low levels of Ca^{2+} may also affect cytoskeletal (31) or membrane components that may be involved in the stabilization of receptor clusters.

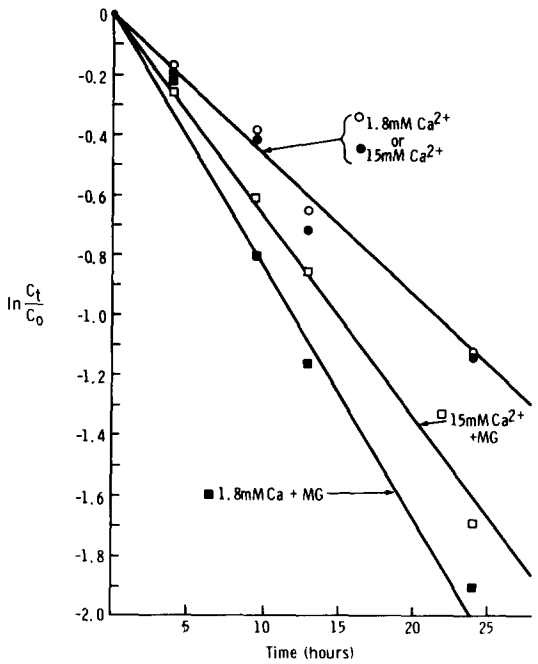

FIGURE 8 The effect of Ca^{2+} concentration on the rate of AChR degradation in the presence of control and absence of myasthenic globulin. Cells were labeled with ^{125}I-BTX, washed, and incubated with: ○, control medium; ●, high Ca^{2+} medium; □, control medium and MG globulin; ■, high Ca^{2+} medium and MG globulin at 37°C. The rate of degradation was determined as described in Materials and Methods. The degradation rate constants expressed as hours^{-1} were: control, 0.046; high Ca^{2+}; 0.036 MG, 0.0084; MG and high Ca^{2+}, 0.066.

The lag periods during which AChR appearance and cluster formation occur at control rates can be accounted for by the transport of a presynthesized pool of AChR to the surface of the myotube (17, 28). Thus, incubation of myotubes in low Ca^{2+} medium does not appear to interfere with receptor transport (28) or cluster formation at early times. It is also possible that the resolution of our technique is not sufficient to detect early changes. Since the present study employed a lower concentration of Ca^{2+} than was used previously, it is possible that the effects of low extracellular Ca^{2+} on the rate of receptor synthesis and degradation are different from those reported (28). To control for this possibility, we repeated these experiments using 2×10^{-5} M Ca^{2+} and found the results to be identical to those previously reported (28).

High concentrations of calcium have the opposite effect on AChR clusters; both the size (Table III) and the rate of appearance (Fig. 5) of AChR clusters are increased in high calcium medium. The changes are probably the result of a redistribution of diffuse AChR and not of an increase in AChR metabolism, since the rates of synthesis and degradation of AChR's in high calcium medium are identical to those of control cultures. The surface distribution of AChR could be altered by high Ca^{2+} concentration in a variety of ways. The concentration of Ca^{2+} has been shown to influence the mobility of membrane lipids which may induce protein aggregation (14, 19). Diffuse AChR are known to migrate in the membrane (4); therefore, an alteration of the mobility of the diffuse receptors could lead to an increase cluster size by increasing the frequency in which diffuse receptors encounter AChR clusters. The increase in cluster size could also explain the decrease in cluster number in high Ca^{2+} medium due to a coalescence of clusters.

Calcium is also known to influence the cytoskeletal and microtrabecular components of cells (20, 31). The cytoskeleton in particular has been postulated to interact with AChR clusters (24, 31). Thus, high concentration of Ca^{2+} may stabilize clusters by enhancing the interaction between AChR clusters and the cytoskeletal framework.

High Ca^{2+} Concentration Partially Protects AChR Clusters from Dispersal by MG

Although the role of Ca^{2+} in antibody- and concanavalin A–induced endocytosis has been investigated in lymphocytes (35, 36) little is known about the effect of Ca^{2+} on the metabolism of AChR in the presence of anti-acetylcholine receptor antibodies. We have previously shown (13) that antiacetylcholine receptor antibodies obtained from patients with myasthenia gravis produce a rapid dispersal of AChR clusters in addition to their well known effect of increasing the rate of AChR turnover (1, 18, 29, 34). High concentrations of Ca^{2+} decrease both the turnover rate and the rate of cluster dispersal of cells treated with MG, but do not alter either parameter in control cultures.

The mechanism by which anti-acetylcholine receptor antibodies increase the turnover rate of acetylcholine receptors is unknown. However, it has been shown that divalent antibodies are necessary to increase receptor turnover, since monovalent Fab fragments do not alter receptor degradation (18). One possible mechanism is that antibodies cross-link receptors (25, 32), stimulating receptor-mediated endocytosis. High concentrations of Ca^{2+} may interfere with this process, resulting in an inhibition of cluster dispersal and a decreased rate of turnover. An analogous effect of Ca^{2+} has been reported for antibody-induced endocytosis in lymphocytes (35, 36). In this case, the intracellular Ca^{2+} concentration was increased by the addition of the Ca^{2+} ionophore A23187. Although we have not measured the intracellular Ca^{2+} concentration of our cells, it is possible that elevated extracellular Ca^{2+} also increases the intracellular Ca^{2+} concentration.

On the basis of available evidence, the factors that have been hypothesized to contribute toward the maintenance of AChR clusters are: (*a*) the rates of synthesis and degradation (13); (*b*) specialized proteins that participate in the anchorage of receptors (8, 24, 30, 31); (*c*) the concentration of Ca^{2+} (6), and the present report); (*d*) extracellular elements such as the basal lamina (11, 21, 26); (*e*) membrane fluidity (10, 19). The mechanism by which Ca^{2+} influences the metabolism of AChR clusters remains to be determined, but it may involve any or all of these factors.

We thank Mannie Steglich and Veronique Dellatre for technical assistance.

This work was supported by National Institutes of Health grant #NS 17876, Muscular Dystrophy Association, and BRSG. Sherry Bursztajn, to whom all correspondence should be addressed, is the recipient of a Research Career Development Award.

Received for publication 16 March 1983, and in revised form 13 September 1983.

REFERENCES

1. Appel, S. H., R. Anwyl, M. W. McAdams, and S. Elias. 1977. Accelerated degradation of acetylcholine receptor from cultured rat myotubes with myasthenic gravis sera and globulins. *Proc. Natl. Acad. Sci. USA.* 74:2130–2134.
2. Anderson, M. J., and M. W. Cohn. 1977. Nerve-induced and spontaneous redistribution of acetylcholine receptors on cultured muscle cells. *J. Physiol. (Lond.).* 268:757–773.

3. Axelrod, D., P. Ravdin, D. E. Koppel, J. Schlissinger, W. W. Webb, E. L. Elson, and T. R. Podleski. 1976. Lateral motion of fluorescently labeled acetylcholine in membranes of developing muscle fibers. *Proc. Natl. Acad. Sci. USA.* 73:4594–4598.
4. Axelrod, D., P. M. Raudin, and T. R. Podleski. 1978. Control of acetylcholine receptor mobility and distribution in cultured muscle membranes: a fluorescence study. *Biochim. Biophys. Acta.* 511:23–38.
5. Axelrod, D. 1980. Crosslinkage and visualization of acetylcholine receptors on myotubes with biotinylated α-bungarotoxin and fluorescent avidin. *Proc. Natl. Acad. Sci. USA.* 77:4823–4827.
6. Birnbaum, M., M. A. Reis, and A. Shainberg. 1980. Role of calcium in the regulation of acetylcholine receptor synthesis in cultured muscle cells. *Pfluegers Archiv. Eur. J. Physiol.* 385:37–43.
7. Bloch, R. J. 1979. Dispersal and reformation of acetylcholine receptors of cultured rat myotubes treated with inhibitors of energy metabolism. *J. Cell Biol.* 82:626–643.
8. Bloch, R. J., and B. Geiger. 1980. The localization of acetylcholine receptor clusters in areas of cell-substrate contact in cultures of rat myotubes. *Cell.* 21:25–35.
9. Bloch, R. J., and J. H. Steinbach. 1981. Reversible loss of acetylcholine receptor clusters at the developing rat neuromuscular junction. *Dev. Biol.* 81:386–391.
10. Bridgman, P. C., and Y. Nakajima. 1981. Membrane lipid heterogeneity associated with acetylcholine receptor particle aggregates in *Xenopus* embryonic muscle cells. *Proc. Natl. Acad. Sci. USA.* 78:1278–1282.
11. Burden, S. J., P. B. Sargent, and U. J. McMahan. 1979. Acetylcholine receptors in regenerating muscle accumulate at original synaptic sites in the absence of the nerve. *J. Cell Biol.* 82:412–425.
12. Bursztajn, S., and G. D. Fischbach. 1984. Evidence that coated vesicles transport acetylcholine receptors to the surface membrane of chick myotubes. *J. Cell Biol.* 98:498–506.
13. Bursztajn, S., J. L. McManaman, S. B. Elias, and S. H. Appel. 1983. Myasthenic globulin enhances the loss of acetylcholine receptor clusters. *Science (Wash. DC).* 219:195–197.
14. Carraway, K. L., R. B. Triplett, and D. R. Anderson. 1975. Calcium promoted aggregation of erythrocyte membrane proteins. *Biochem. Biophys. Acta.* 379:571–581.
15. Daniels, M. P., and Z. Vogel. 1975. Immunoperoxidase staining of α-bungarotoxin binding sites in muscle endplate shows distribution of acetylcholine receptors. *Nature (Lond.).* 254:339–341.
16. Deutsch, H. F. 1967. Preparation of immunoglobulin concentrates. *Methods Immunol. Immunochem.* 1:315–321.
17. Devreotes, P. N., and D. M. Fambrough. 1975. Acetylcholine receptor turnover in membranes of developing muscle fibers. *J. Cell Biol.* 65:335–358.
18. Drachman, D. B., C. W. Angus, R. N. Adams, J. Michelson, and G. J. Hoffman. 1978. Myasthenic antibodies cross-link acetylcholine receptors to accelerate degradation. *N. Engl. J. Med.* 298:1116–1122.
19. Elgsaeter, A., D. M. Sholton, and D. Branton. 1976. Intramembrane particle aggregation in erythrocyte goasts. II. The influence of spectrin aggregation. *Biochem. Biophys. Acta.* 426:101–122.
20. Ellisman, M. H., and K. R. Porter. 1980. Microtrabecular structure of the axoplasmic matrix: visualization of cross-linking structures and their distribution. *J. Cell Biol.* 87:464–479.
21. Fambrough, O. M., E. K. Bayne, J. M. Gardner, M. J. Anderson, E. Wakshull, and R. L. Rotundo. 1982. Monoclonal antibodies to skeletal muscle cell surface. *In* Neuroimmunology. J. Brodus, editor. Plenum Press, New York. pp. 49–90.
22. Fischbach, G. D., and S. A. Cohen. 1973. The distribution of acetylcholine sensitivity over uninnervated and innervated muscle fibers grown in cell culture. *Dev. Biol.* 31:147–162.
23. Frank, E., and G. D. Fischbach. 1979. Early events in neuromuscular junction formation in vitro. Induction of acetylcholine receptor clusters in the post-synaptic membrane and morphology of newly formed synapses. *J. Cell Biol.* 83:143–158.
24. Hall, Z. W., B. W. Lubit, and J. H. Schwartz. 1981. Cytoplasmic actin in post-synaptic structures at the neuromuscular junction. *J. Cell Biol.* 90:789–792.
25. Lennon, V. A. 1978. Immunofluorescence analysis of surface acetylcholine receptors of muscle: modulation by auto-antibodies. *In* Cholinergic Mechanisms and Psychopharmacology. D. J. Jender, editor. Plenum Press, New York. pp. 77–92.
26. McMahan, U. J., P. B. Sargent, L. L. Rubin, and S. J. Burden. 1980. Factors that influence the organization of acetylcholine receptors in regenerating muscle are associated with the basal lamina in the neuromuscular junction. *In* Ontogenisis and Functional Mechanisms of Peripheral Synapses. J. Taxi, editor. Elsevier/North Holland, Amsterdam. pp. 345–354.
27. McManaman, J. L., J. C. Blosser, and S. H. Appel. 1982. Inhibitors of membrane depolarization regulate acetylcholine receptor synthesis by a calcium-dependent, cyclic nucleotide-independent, mechanism. *Biochem. Biophys. Acta.* 720:28–35.
28. McManaman, J. L., J. C. Blosser, and S. H. Appel. 1981. The effect of calcium on acetylcholine receptor synthesis. *J. Neurosci.* 1:771–776.
29. Merlie, J. P., S. Heinemann, and J. M. Lindstrom. 1979. Acetylcholine receptor degradation in adult rat diaphragms in organ culture and the effect of acetylcholine receptor antibodies. *J. Biol. Chem.* 254:6320–6327.
30. Nakajima, Y., and P. C. Bridgman. 1981. Absence of filipinsterol complexes from the membranes of active zones and acetylcholine receptor aggregates at frog neuromuscular junctions. *J. Cell Biol.* 88:453–458.
31. Prives, J., A. B. Fulton, S. Penman, M. P. Daniels, and C. N. Christian. 1982. Interaction of the cytoskeletal framework with acetylcholine receptor on the surface of embryonic muscle cells in culture. *J. Cell Biol.* 92:231–236.
32. Pumplin, D. W., and D. B. Drachman. 1983. Myasthenic patients' IgG causes redistribution of acetylcholine receptors: freeze-fracture studies. *J. Neurosci.* 3:576–584.
33. Ravdin, P., and D. Axelrod. 1977. Fluorescent tetramethyl rhodamine derivatives of α-bungarotoxin, preparation, separation and characteriziation. *Anal. Biochem.* 80:585–592.
34. Reiness, C. G., C. B. Weinberg, and Z. W. Hall. 1978. Antibody to acetylcholine receptor increases degradation of junctional and extrajunctional receptors in adult muscle. *Nature (Lond.).* 274:68–70.
35. Schreiner, G. F., and E. R. Unanue. 1976. Calcium-sensitive modulation of Ig capping: evidence supporting a cytoplasmic control of ligand-receptor complexes. *J. Exp. Med.* 143:15–31.
36. Schreiner, G. F., and E. R. Unanue. 1976. Membrane and cytoplasmic changes in B lymphocytes induced by ligand-surface immunoglobulin interaction. *Adv. Immunol.* 24:37–164.
37. Shainberg, A., S. A. Cohn, and P. G. Nelson. 1976. Induction of acetylcholine receptors in muscle cultures. *Pfluegers Arch. Eur. J. Physiol.* 361:255–261.
38. Stya, M., and D. Axelrod. 1983. Diffusely distributed acetylcholine receptors can participate in cluster formation on cultured rat myotubes. *Proc. Natl. Acad. Sci. USA.* 80:449–453.
39. Vogel, Z., A. J. Sytkowski, and M. W. Niremberg. 1972. Acetylcholine receptors of muscle growth in vitro. *Proc. Natl. Acad. Sci. USA.* 69:3180–3184.
40. Yaffe, D. 1969. Cellular aspects of muscle differentiation *in vitro. Curr. Top. Dev. Biol.* 4:37–77.
41. Ziskind-Conhaim, L., and J. I. Bennett. 1982. The effects of electrical inactivity and denervation on the distribution of acetylcholine receptors in developing rat muscle. *Dev. Biol.* 90:185–197.